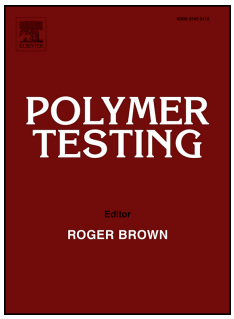

Bio-based polybenzoxazine composites for oil-water separation, sound absorption and corrosion resistance applications

Arumugam Hariharan, Pichaimani Prabunathan, Ammasai Kumaravel, Manickam Manoj, Muthukarupan Alagar

PII: S0142-9418(19)32166-X

DOI: https://doi.org/10.1016/j.polymertesting.2020.106443

Reference: POTE 106443

To appear in: *Polymer Testing*

Received Date: 20 November 2019

Revised Date: 11 February 2020

Accepted Date: 15 February 2020

Please cite this article as: A. Hariharan, P. Prabunathan, A. Kumaravel, M. Manoj, M. Alagar, Bio-based polybenzoxazine composites for oil-water separation, sound absorption and corrosion resistance applications, *Polymer Testing* (2020), doi: https://doi.org/10.1016/j.polymertesting.2020.106443.

CRediT authorship contribution statement

Arumugam Hariharan : Conceptualization, Methodology, Investigation, Visualization, Data curation, Writing- original draft preparation, Writing- reviewing and editing.

Pichaimani Prabunathan: Oil-water separation methodology, Writing- reviewing and editing.

Ammasai Kumaravel: Electrochemical workstation methodology.

Manickam Manoj: Resources, Validation, Software.

Muthukarupan Alagar : Supervision.

Bio-based polybenzoxazine composites for oil-water separation, sound absorption and corrosion resistance applications.

Arumugam Hariharan[a], Pichaimani Prabunathan[a], Ammasai Kumaravel[b], Manickam Manoj[a], Muthukarupan Alagar[a]*

[a]Polymer Engineering Laboratory, PSG Institute of Technology and Applied Research, Neelambur, Coimbatore - 641 062, India.
[b]Department of Chemistry, PSG Institute of Technology and Applied Research, Neelambur, Coimbatore - 641 062, India.
*Corresponding author: mkalagar@yahoo.com

Abstract

In the present work, an attempt has been made to develop bio-based composites using cardanol and eugenol based benzoxazine matrices with bio-silica as well as natural fibrous materials (coir felt, kapok fabric, jute felt and rice husk) as reinforcements. The bio-composites developed were studied for different applications viz., dielectric, water repellent, oil-water separation, sound-absorption including corrosion resistance use. Among the bio-silica reinforced benzoxazine composites, 7 wt% bio-silica reinforced cardanol composites possesses the highest value of water contact angle (147˚) and the lowest value of dielectric constant (2.0) than those of other bio-silica reinforced composites. Further, the cotton fabric was coated with cardanol and eugenol based polybenzoxazines separately, whose values of water contact angles are found to be 159˚ and 157˚ with oil-water separation efficiency as 96% and 95 % respectively. Furthermore, the cardanol based benzoxazine was separately reinforced with jute felt, coir felt, kapok fabric and rice-husk. The corresponding sound absorption efficiency was found to increase in the following order, Neat polybenzoxazine < rice husk < coir felt < kapok fabric < jute felt. Data resulted from corrosion studies, it was noticed that the mild steel specimen coated with bio-based benzoxazine matrices and bio-silica reinforced benzoxazine composites coated specimens exhibit an excellent resistance to corrosion. Data resulted from different studies, it is suggested that the cardanol and eugenol based bio-composites can be considered as an effective materials for microelectronics insulation, water repellent, oil-water separation, sound absorption and corrosion resistant applications.

Key words: bio-benzoxazines, bio-silica, natural fibers, bio-composites, water contact angle, dielectric contact, oil-water separation, sound absorption coefficient, corrosion resistance.

Introduction

Development of commercial materials from renewable resources become major thrust area for researchers around the world, since it alleviates most of the environmental problems. A variety of chemicals, monomers, polymers and other products have been prepared from bio-source materials, namely wood, proteins, cellulose, lignin, tannins, starch, chitin, chitosan, etc, have been used for different industrial and engineering applications.[1–15] Among the bio-based products derived, bio-phenols viz., cardanol from cashew nut shell liquid (CSNL) and eugenol from clove oil are considered to be the most important precursor materials and are widely used for the preparation of polymers and polymer based products like epoxy, cyanate ester, benzoxazine, etc.[16,17] In the recent past, researchers around the world have extensively studied the benzoxazine based materials using variety bio-precursor materials for different applications. The synthesis of benzoxazines were carried out through Mannich condensation using phenolic derivatives, formaldehyde and amines.[18] Benzoxazines possess an enhanced thermal properties, improved flame resistance, good mechanical performance, flexible molecular design and near zero shrinkage during curing. Our group have been actively involved in the development of different types of benzoxazines for various engineering applications and reported elsewhere.[18–22][23]

Recently our research group have developed and published bio-based benzoxazines using renewable bio-resource raw materials namely cardanol and eugenol with aniline, N, N-dimethyl amino propyl amine (DMAPA) and caprolactam modified DMAPA separately.[23] The graphene reinforced eugenol based polybenzoxazine composites were also prepared by incorporating varying weight percentages (1, 3, 5, 7, and 10 wt %) of graphene oxide to obtain hybrid nanocomposites for high dielectric application[19]. Further, prepared cardanol based benzoxazines were reinforced with varying weight percentages (1, 3, 5 and 10 wt %) of bio-silica derived from rice husk to obtain hybrid composites for low dielectric application [23]. We have also prepared the bio based polybenzoxazine-silica hybrid through in-situ sol–gel method for high thermal and flame retardant applications [24]. Furthermore, the bio-silica reinforced eugenol based polybenzoxazine composites have been developed for low k application and reported.[25]

In the present work an attempt has been made to prepare two types of bio-benzoxazines based on cardanol and eugenol separately using furfuryl amine and paraformaldehyde under appropriate experimental conditions and their properties were characterized using different analytical methods. Both bio-benzoxazines have been composited with bio-mass derived reinforcements, such as rice husk ash bio-silica, natural fibers (rice husk, coir felt, kapok fabric, jute felt) and cotton fabrics for various industrial applications. The varying weight percentages of bio-silica reinforced bio benzoxazine composites have been studied for their insulation behavior and corrosion resistant efficiency. The bio-based benzoxazines coated cotton fabrics were studied for oil-water separation behavior. Further, cardanol based benzoxazine was reinforced with natural fiber reinforcements namely rice-husk, coir felt, jute felt and kapok and the composites resulted were tested for their sound absorption behavior. The present study utilizes the fully bio-based benzoxazines and bio-based reinforcements to develop composites for some of the versatile industrial applications (Fig. 1). Data obtained from different studies are discussed and reported.

Experimental

Materials

Cardanol was obtained from Satya cashew products, Chennai. Eugenol, paraformaldehyde, and anhydrous sodium sulphate (Na_2SO_4) were obtained from Spectrochem, India. Furfuryl amine was purchased from Sigma Aldrich. Ethyl acetate and sodium hydroxide has received from SRL, India. Glycidoxypropyltrimethoxysilane (GPTMS) was obtained from Sigma Aldrich. Natural fibers, cotton fabric and rice husk have been collected from local source Tamilnadu, India.

Synthesis of the benzoxazine monomers.

Separately 0.1mol of cardanol (C) and eugenol (E) reacted with 0.1mol of furfuryl amine (f) and 0.2mol of paraformaldehyde, which were placed in a 250 ml three-neck round bottomed flask equipped with magnetic stirrer, thermometer and without solvent. The reaction mixture was heated under constant agitation at 100 ^{o}C for 3-4 h. The crude products obtained from the reaction were (Schemes 1 and 2) diluted separately using ethyl acetate and then thoroughly washed with distilled water. The organic phase was separated and dried with anhydrous sodium

sulfate and filtered. The solvent was removed under vacuum distillation. A consistent amount of benzoxazine was isolated and characterized by FT-IR (**Fig. S1**) and ^{1}H NMR (**Fig. S2a-b**.), spectroscopic techniques.

Preparation of neat benzoxazine matrices and bio-silica reinforced composites

The polymerization of benzoxazines was carried out via thermal ring opening mechanism. Bio based benzoxazine (eugenol as well as cardanol benzoxazines) monomers are taken in a petri dish separately and dried well at 60 ^{o}C for 6 h. Further, before curing the monomers were subjected to 80 °C for 8 h to stabilize and to remove the traces of moisture if any present. After the stabilization, the temperature was raised to 250 °C at a rate of 20 °C per hour. The temperature was maintained for another 3 h in order to achieve the completion of curing process. The formation of polybenzoxazines with cross-linked network are shown in Schemes 3 and 4.

The formation of bio-silica[23,25] reinforced bio-based benzoxazines (Poly(C-f) and Poly(E-f)) are presented in Schemes 5 and 6 respectively. The preparation of GPTMS functionalized bio-silica has been given in the supporting information (Scheme S1). In brief, 1, 3, 5 and 7 wt% of bio-silica were separately reinforced with C-f and E-f benzoxazine monomers and stirred for 1 h to obtain the homogeneous blends. The blends obtained were cured in a similar manner as carried out for the preparation of neat matrices.

Measurements

FTIR spectra measurements were carried out with Agilent Cary 630 FTIR Spectrometer. NMR spectra were obtained with Bruker (400 MHz) using dimethylsulfoxide (d6-DMSO) as a solvent and tetramethylsilane (TMS) as an internal standard. DSC measurements were recorded using NETZSCH STA 449F3 under N_2 purge (60 mL min^{-1}) at scanning rate of 10 ˚C min^{-1}. Thermogravimetric analysis (TGA) was obtained using NETZSCH STA 449F3 taking 5 mg of sample under N_2 flow (260 mL min^{-1}) and controlling the heating rate at 20 ˚C min^{-1}. The dielectric constant was determined with help of an impedance analyzer (Solartron impedance analyzer 1260, UK) at room temperature using platinum electrode from 1 Hz to 1MHz. The surface overview of the composite films was identified from an FEI QUANTA 200F high-resolution scanning electron microscope (HRSEM). Contact angle measurements were obtained

using a Kwoya goniometer with 5µl of water as probe liquid. HR-TEM images were captured using a TECNAI G2 S-Twin high resolution transmission electron microscope, with an acceleration voltage of 150 kV. TEM samples were prepared by dispersing the composites in ethanol, mounting them on carbon-coated Cu TEM grids and dried at 30 ˚C for 24 h to obtain a film of 100 nm in size. The benzoxazines coated mild steel plates were tested for their corrosion protection behavior on mild steel in 3.5% sodium chloride solution. The corrosion resistant behavior of mild steel specimens were carried out using open-circuit potential (OCP), electrochemical impedance spectroscopy (EIS) and potentiodynamic polarisation. Analysis of sound absorption (acoustic behavior) was carried out using the impedance tube method. The sound absorption coefficient (SAC) of fibre reinforced composites was measured through a transfer function technique with the impedance tube facilities [manufactured by Bruel & Kjaer 3160-A-042, Denmark]. The SAC is defined as the ratio of the absorbed sound energy and the incident sound energy. The measurements were conducted according to ISO10534-2 standard at lower to higher frequencies from 4 to 6400 Hz at ambient temperature and at least two specimens were tested for each type of samples. Two types of SW422 and SW477 impedance tubes with diameters of 100 mm and 30 mm for measuring frequencies from 0–1600 Hz and 4–6300 Hz, respectively were used. Samples were backed up by a rigid wall which reflected all the incoming sound energy. Two microphones were mounted at the wall of the tube to measure the sound pressure. Hence, if the incident sound energy is known and the transmission sound energy can be measured with the aid of the transfer function and the sound energy absorbed by the materials will be calculated. The tensile properties of the fabrics were measured using a universal testing machine (Tensile Tester Z10 of Zwick/Roell, Germany), with a constant rate of extension. The test was done according to ASTM standard D5035-11 (Reapproved 2015). The porosity of the fabrics were measured using capillary flow analysis from Porous Materials, Inc. Analytical Services, USA.

Results and discussion

The cardanol and eugenol based benzoxazines (C-f and E-f) were prepared through Mannich condensation reaction of cardanol and eugenol separately mixed with stoichiometric quantities of furfuryl amine and paraformaldehyde at appropriate conditions in the absence of any solvents as shown in Schemes 1 and 2 respectively. The benzoxazine monomers obtained

were characterized by different analytical techniques.The molecular structures of cardanol-furfuryl amine (C-f) and eugenol-furfuryl amine (E-f) based benzoxazine monomers were confirmed by FT-IR and ^{1}H NMR spectral analysis. The thermal behaviour of the synthesized benzoxazines has been studied by TGA and DSC analysis. The data obtained from different analysis are discussed.

The bands appeared in FT-IR spectrum (Fig. S1) at 1242 cm^{-1} and 1090 cm^{-1} were attributed to the asymmetric and symmetric stretching vibrations of C-O-C bond in the benzoxazine respectively. The peak appeared at 1152 cm^{-1} represents the asymmetric stretching of C-N-C. Similarly, the appearance of bands at around 940 cm^{-1} and 1492 cm^{-1} correspond to a tri-substituted benzene ring which confirms the formation of benzoxazine ring. Further, the band appeared at around 3009 cm^{-1} corresponds to C-H stretching vibrations of benzene ring. Characteristic bands appeared at 2925 and 2853 cm^{-1} are corresponds to the asymmetric and symmetric stretching vibrations of CH_2 of oxazine ring as well as alkyl side chain of cardanol moiety. The ^{1}H NMR spectrum was also found to be consistent with the proposed benzoxazine structure (Fig. S2a-b); The linear aliphatic chain and methyl (CH_3-) and methylene(-CH_2-) group signals are appeared at 0.9-3.8ppm. it confirms the meta substituted aliphatic chain of cardanol moiety. Further, shows two typical singlets centered respectively at 5ppm (O-CH_2-N) for hydrogen atoms of the nitrogen and oxygen bonded methylene groups, and around 4ppm (Ar-CH_2-N) for hydrogen atoms of the nitrogen and aryl bonded methylene groups respectively. The multiplet signals were appear at 6.5-7.5.0ppm, which confirms the aryl protons. In Fig. S2a-b 6ppm and 7.8ppm are confirm the presence of furan ring substitution. Specifically in Fig.2b, multiplet signals at 5ppm and 5.9ppm are represent the allyl substitution and a singlet signal absorbed at 3.8ppm which confirms the *ortho* substituted methoxy group protons.

The polymerization process involved to obtain polybenzoxazines is based on the ring opening of benzoxazine monomer. Benzoxazine monomer was polymerized with rice-husk ash silica in order to utilize for low k application and corrosion resistance application. Further, the bio-benzoxazine composites have been fabricated with different bio-reinforcements (jute felt, kapok nonwoven fabric, rice husk) for sound absorption, in addition to the benzoxazine coated cotton fabrics for oil-water separation application.

Thermal behavior

DSC analyses infer that the polymerization temperature (Tp) of benzoxazine monomers (Fig. S3). The Tp of C-f benzoxazine monomer is observed at 259^{o}C with single exothermic peak, whereas that of E-f benzoxazine monomer exhibits dual exothermic peaks at 241 and 287 ^{o}C. The polymerizations of benzoxazines proceed with the cleavage of oxazine rings, which were ascertained from the disappearance of bands at 940 cm^{-1} (Fig. S9a-b). Among the polybenzoxazine (poly(C-f) and poly(E-f)) composites studied in the present work, cardanol based bio-silica reinforced composites possesses better stability to towards thermal decomposition than that of eugenol based bio-silica reinforced composites.[26] This may be explained due to the complexity and entanglement of long chain associated with cardanol moiety. Thermal stability behavior of benzoxazine composites obtained from thermogravimetric analysis are presented in Fig. S10a-b and Table 1. It was observed from TGA data that thermal stability of functionalized bio-silica reinforced composites has been enhanced according to the weight percentage concentration. The maximum degradation (T_d) temperature obtained for neat matrix, 1wt%, 3wt%, 5wt% and 7wt% bio-silica reinforced poly(C-f) composites are 463, 467, 470, 474 and 478 ^{o}C respectively. The char yield of poly(C-f) and bio-silica 1wt%, 3 wt%, 5 wt% and 7 wt% reinforced poly(C-f) composites at 800°C was observed to be 4, 6, 10, 11 and 12% respectively. Similarly, poly(E-f) and bio-silica 1wt%, 3 wt%, 5 wt% and 7 wt% reinforced poly(E-f) composites trend of char yield was observed about 42, 45, 46, 51 and 53%.

Generally, it is known that benzoxazine cationic ring opening polymerization will occur at *ortho* and *para* position.[27] Cardanol based benzoxazine matrix have better thermal degradation maxima than that of eugenol based benzoxazine matrix due to the availability of more favored ortho and para position for cross linkage of polymer matrix (Fig. S11), In case of eugenol, *ortho* and *para* postions are occupied by methoxy and allyl groups respectively. Hence, only the less favored meta-position is available for polymerization. As a result eugenol based benzoxazine degradation maxima occurred at lower temperature than that of cardanol benzoxazine. Even though, the *para* substituted allylic group of eugenol may expected to undergo Diels-Alder reaction with furfuryl group,[28] it helps only to improve the char yield. From our previous reports, it was observed that the aniline, stearyl amine and dimethylaminopropyl amine (DMAPA) based eugenol benzoxazine polymer matrices possess

lower char residue than that of furfuryl amine and eugenol based benzoxazine matrix.[23,29] This may be due to the extension of Diels-Alder polymerization (Scheme 4).

Morphological behavior

The XRD diffractogram of bio-silica reinforced cardanol and eugenol based polybenzoxazine composites are presented in Fig. 2a-b. A peak appeared at 2θ = 20°, infers the that the composites and matrices are in amorphous nature. Also confirms the distribution of silica in homogeneous manner. In addition microscopic images observed from SEM analysis also confirms the uniform and homogeneous distribution of bio-silica throughout the benzoxazine matrices of both poly(C-f) and poly(E-f). The morphology of neat matrices are observed to be smooth, whereas that of the bio-silica reinforced composites (Fig. 3 and 4), show crack propagated and rough surfaces. The formation of rough surface is highly desirable for coating application, which desirably provides superhydrophobic behavior with low surface free energy.

Furthermore, in order to ascertain the distribution of bio-silica in the bio benzoxazine (Poly(C-f), Poly(E-f)) matrix, the HR-TEM analysis was carried out and the images obtained are presented in Fig. 5 and 6, respectively. 3 wt %, 5 wt % and 7wt % of bio-silica reinforced benzoxazine (POLY(C-F), Poly(E-f)) were taken as representative samples for TEM analysis. The TEM images of 3 wt % (Fig. 5a and 6a), 5 wt % (Fig. 5b and 6b) and 7 wt % (Fig. 5c and 6c) bio-silica reinforced nanocomposites show uniform dispersion of silica in the Poly(C-f), Poly(E-f) matrices. The distributions of bio-silica (F-SiO_2) are observed to be homogenous even at higher weight percentages. This phenomenon influences and contributes to the lower value of dielectric constant in addition to an enhancement of high thermal stability and enhanced water contact angle properties achieved with homogeneity of bio-silica. Among the hybrid composites studied, the 7 wt % F-SiO_2/Poly(C-f) and poly(E-f) nanocomposites can be considered as better material for high performance microelectronics insulation applications.

Bio-silica reinforcement in benzoxazine matrices (Poly(C-f) and Poly(E-f)) influences the enhancement of thermal behavior and the formation of covalent bonding network structure. Further, the bio-silica reinforcement also contributes to the development of smooth surface, which in turn makes the composites surface become hydrophobic nature according to the nature of benzoxazine matrix and weight percentage of bio-silica reinforcement.

Dielectric behavior

The value of dielectric constant (k) of neat benzoxazine matrix of poly(C-f) is 3.6 (Fig. S12 and Table 1). The values of dielectric constant of bio-silica reinforced poly(C-f) benzoxazine composites are decreased according to the weight percent of bio-silica (1, 3, 5 and 7 wt%). Among the bio-silica composites studied, cardanol based bio-composites possesses the lower values of dielectric constant (k=2.0) than that of poly(E-f) based composites (k = 2.1(Fig S12 and Table 2)) due to the long alkyl chain moiety in combination with the presence of bio-silica network. The presence of long alkyl chains in between the matrices pave the formation of free space with air voids (k=1), which in turn influences in reducing the value of dielectric constant of the matrix.

Surface behavior

The value of water contact angle of poly(C-f) and poly(E-f) polybenzoxazines are 98^{o} and 92^{o} respectively, whereas the values of 1wt%, 3 wt%, 5 wt% and 7 wt% of bio-silica reinforced with poly(C-f) composites are 113^{o}, 124^{o}, 131^{o} and $147^{o,}$ respectively (Fig. 7). Similarly, the contact angle values of 1 wt%, 3 wt%, 5 wt% and 7 wt% of bio-silica reinforced Poly(E-f) composites are 96^{o}, 105^{o}, 118^{o} and $128^{o,}$ respectively (Fig. 8). Among the benzoxazine composites studied in the present work, poly(C-f)/bio-silica composites possess higher values of contact angle than that of poly(E-f)/bio-silica composites. The enhanced hydrophobic behavior exhibited by poly(C-f)/bio-silica composites may be explained due to the presence of long aliphatic chain of cardanol moiety with low polar siloxane moiety contributed by bio-silica network, in addition to the inherent intra-molecular hydrogen bonding present in the benzoxazine system.

Corrosion studies using EIS measurements

The EIS was carried out to assess the corrosion resistant behavior of the poly(C-f) and poly(E-f) matrices and bio-silica reinforced composites coated on the mild steel with surface area of specimen having $2cm^2$. The coated specimens were immersed in 3.5% NaCl solution for different period of time intervals and tested. The OCP values obtained were plotted against period of immersion. The change in the values of OCP was monitored over a period of 200 min

for bare mild steel specimen, specimen coated with 7wt% bio-silica reinforced Poly(C-f) and Poly(E-f) composites are presented in Fig. 9. From the Figure, it was noticed that the OCP values of the coated specimens were shifted significantly to the anodic direction when compared with that of the bare mild steel specimen. It can also be seen that OCP values of the benzoxazine coated specimens are much lower when compared to that of bare mild steel specimen. The OCP shift toward positive values infer high the corrosion resistance offered by the benzoxazine coatings.[30,31] This effect is more pronounced when bio-silica were reinforced into the coatings. Among the two different benzoxazine composites coated specimens, bio-silica reinforced poly(E-f) composites coated specimens show more anodic shift of OCP values due to the formation of firm adherent film, which in turn contributes to lower permeability of the corrosion medium into the film.[32]

The EIS was used to evaluate the barrier properties of the poly(C-f) and Poly(E-f) coatings and the effect of incorporation of bio-silica on the corrosion resistance of MS. Nyquist plots from EIS measurements for neat benzoxazine matrices and bio-silica reinforced composites coated and uncoated mild steel specimens in 3.5% NaCl solution are presented in Fig. 10a-b. Nyquist plots have only one capacitive semicircle for all the specimens represent the presence of only one time constant.[33] Hence, fitting of all EIS data was done using simple equivalent circuit model (Fig. 11). The equivalent circuit was used to evaluate the corrosion resistance data, where Rs is the solution resistance, Rct is the charge transfer resistance and Qc is the double layer capacitance.

Superimposition of the experimental data has been done using this equivalent circuit and corrosion parameters were calculated. Rs is the resistance of the solution between the working electrode and the counter electrode. Rs values are not only depending on the ionic conductivity of the solution but also depending on the geometrical area of the electrode. Rs values are not an important data while studying the corrosion property of the film because it does not yield any information about the coating. Hence, Rct values are used to measure the resistance of the electron transfer across the metal-solution interface, which is inversely proportional to the corrosion rate of the metal. The calculated values of the corrosion parameters from EIS measurements are presented in Table 3. Rct values of poly(C-f) and poly(E-f) coated specimens are higher than that of bare mild steel (MS). In order to improve the corrosion resistance

behavior of poly(C-f) and poly(E-f) coatings, the bio-silica was reinforced in to the benzoxazine matrix. When the content of bio-silica were increased from 1wt% to 7wt%, into the matrix, the increase in Rct and decrease in double layer capacitance values were observed. It ascertains the improved corrosion resistance of coatings ,which may explained due to the reduction of pores/cavities present in the coating which could be occupied by the bio-silica.[34–37] It was well known that, all the organic coatings are not completely impenetrable for long time, their barrier properties could decrease when immersion time increases because of the water/corrosion medium penetrates into the coatings. For bare MS, the corrosion medium had a direct contact with the metal surface which influence to the formation of many electro active sites and in turn led to corrosion in the presence of moisture and oxygen. Bio-silica containing polymer coatings prevent the diffusion of oxygen and aggressive medium into the polymer matrix due to the formation of highly cross- linked –Si-O-Si- network. Further, the values of contact angle of coatings used in the present work, infer that all the bio-silica reinforced coatings are hydrobhobic nature, which in turn effectively prevents the wetting of the surface of coated specimens.[31] Among the varying weight percentage of bio-silica reinforced benzoxazine composites 7 wt% bio-silica benzoxazine composites offer a better corrosion resistance due to the presence of aliphatic side chain and nitrogen atoms. Among the two different bio-composites (poly(C-f)/bio-silica and poly(E-f) /bio-silica) used in the present work, The bio-silica reinforced poly(E-f) composites exhibits better correction resistance than that of poly(C-f) bio-silica reinforced composites.

Fig. 12 show the Tafel plots of uncoated and coated MS specimens. The corrosion rate (CR) was calculated using Icorr values using the equation (1)

$$CR = MI_{corr} / \rho nF \text{……..(1)}$$

Where M is the molecular mass of copper(58.69 g mol^{-1}), Icorr is the corrosion current density(Acm^{-2}), F is the Faradays constant (96500 A s mol^{-1}), ρ is the density of the mild steel specimen (7.85 g cm^{-3}), and the number of electrons transferred during corrosion reaction is assumed to be 2.[34]

The E_{corr} values of bio-silica reinforced polybenzoxazine composites coated specimens increased anodically and I_{corr} values of the coated specimens decreased with the increasing weight percentage of bio-silica indicating that the improved corrosion resistance of the coated

specimens. The improved corrosion resistance may be due to the reinforcement of bio-silica nano-particles suppressed the anodic corrosion reactions (Table 3).[38] The Poly(E-f) with 7wt% bio-silica coating shows better positive shift in terms of E_{corr} value and lower corrosion current. The results obtained from the Tafel method supports the results from EIS and OCP studies.

Oil-water separation studies of benzoxazine coated fabrics.

The preparation method of poly(C-f) and poly(C-f) coated cotton fabrics were given in the supporting information. The thermally cured 5cm diameter sized cotton fabrics coated with benzoxazines possess an excellent hydrophobic behavior. The polybenzoxazines coated cotton fabric was used for further studies and compared with neat fabric. It was observed that the water contact angle values (Fig. 13) obtained for thermally cured cotton fabric coated with 5 wt% benzoxazines (Poly(C-f) and Poly(E-f)) are 157^o and 159^o, respectively, which is higher than that of cotton fabric coated with benzoxazine obtained from bisphenol-A and aniline (132^o)[39]. The higher values of contact angle obtained for cardanol and eugenol based benzoxazines coated fabrics may be explained due to the presence of long alkyl chain in cardanol and alkoxy and allyl moiety present in eugenol which contributes to an enhanced hydrophobic behaviour. Further the cotton fabrics coated with benzoxazines (Poly(C-f) and Poly(E-f)) has been tested for their oil-water separation behavior by utilizing them as filtration substrate. The higher water contact angle observed for benzoxazine coated cotton fabrics have been utilized for further studies. The porous size of cotton fabric was found to be 28.9 microns before coating. The average porosity of poly(C-f) and poly(E-f) coated cotton fabric were checked and found to be 25.8 and 26.1 microns respectively. The tensile strength of (warp and weft) non coated fabric, 5 wt% poly(C-f) and poly(E-f) coated fabrics were studied. The tensile strength of 5 wt% poly(C-f) and poly(E-f) coated fabrics have been observed higher than that of non-coated cotton fabrics (Table 5).

The oil-water mixture was prepared by mixing the engine oil (20W40, density 0.88 $g.cm^{-3}$) and distilled water in 1:2 volumes. The density of the oil is lesser than water. So oil phase will be in the top of the aqueous phase. In order to bring the oil phase down, a high density non-polar solvent dichloromethane (density 1.325 $g.cm^{-3}$) has been added to oil-water mixture. Then the separation of oil was carried out using benzoxazine coated fabrics at room temperature without applying any external force as presented in Fig. S14. From the oil-water separation the separation

efficiency was calculated using equation 2 and found to be 96% and 95% respectively for Poly(C-f) and Poly(E-f) coated cotton fabrics. Similarly the flux values were calculated using equation 3 for both Poly(C-f) and Poly(E-f) coated cotton fabrics. The calculated flux values are 573 and 553 L/m^{2}h, respectively for Poly(C-f) and Poly(E-f) coated cotton fabrics.

$$\text{Separation Efficiency \%} = \frac{Volume\ of\ the\ oil\ after\ separation}{Volume\ of\ the\ oil\ before\ separation} \times 100 \quad \text{.....(2)}$$

$$\text{Flux} = \frac{Volum,e\ of\ the\ permeated\ oil}{Area\ of\ the\ fabric\ X\ time\ for\ separation} \quad \text{.....(3)}$$

Further, in order to ascertain the performance behavior of oil-water separation efficiency of cotton fabrics coated separately with benzoxazines (Poly(C-f) and Poly(E-f)), the experiment was repeated 10 times after washing and drying the fabrics at end of the each experiment. From the oil separation experiments carried out after 10 cycles using the fabrics, it was found to be the separation efficiency of fabrics are found to be about 92 % and 91 % respectively (Fig. 14a and 15a). Similarly, the flux values obtained after 10 cycles are found to be 506 and 501 L/m^{2}h respectively (Fig. 14b and 15b).

In addition, the super-hydrophobic benzoxazine coated cotton fabric was tested to absorb the engine oil (20W40) and it was noted that one gram of the benzoxazine coated cotton was able to absorb the engine oil weight of around 50 times that of its own weight. The details of oil absorption experiment carried out are given in Fig. S15.

Sound absorption performance of bio-composites.

The standing wave is generated in the impedance tube (Fig. S16) and used to analyse the sound absorption behavior of composites (Fig. S17) developed. The absorption of sound energy by the different fiber reinforced cardanol based benzoxazine composites are presented in Fig. 16. Data obtained from sound absorption studies conducted at 1600 Hz, it was observed that the sound absorption of efficiency of neat cardanol benzoxazine matrix, jute felt, coir felt, kapok fabric and rice-husk reinforced Poly(C-f) composites are 0.03, 0.032, 0.05, 0.05 and 0.07 respectively. Similarly , the sound absorption efficiency conducted at 6300 Hz for neat benzoxazine matrix, jute felt, coir felt, kapok fabric and rice-husk reinforced cardanol benzoxazine composites are 0.46, 0.79, 0.70.0.74 and 0.68 respectively.

Data obtained from the sound absorption studies carried out over the frequency range of 1000Hz to 6300 Hz for different natural fiber reinforced cardanol based benzoxazine composites are presented in Table S1. From the Table S1, it can be seen that the sound absorption coefficient increases with increasing frequency from 1000 Hz to 6300 Hz irrespective of reinforcement. The fiber reinforced bio-composites possess higher sound absorption coefficient (SAC)[40] than that of neat benzoxazine matrix. However, among the reinforcements used in the present study, jute felt reinforced cardanol benzoxazine composites possess the better sound absorption efficiency than that of other fiber reinforced composites. The sound absorption coefficient of fiber reinforced benzoxazine composites follow the order,

Neat benzoxazine matrix < rice husk< coir felt< kapok fabric < jute felt

Conclusion

The bio-mass composites based on benzoxazines of cardanol, eugenol, furfuryl amine, bio-silica and natural fibrous materials (rice husk, coir felt, kapok fabric, jute felt, and cotton fabric) were prepared and characterized by different analytical techniques. Among the bio-silica reinforced benzoxazine composites studied, 7wt% bio-silica reinforced cardanol benzoxazine composites possesses the higher value of water contact angle (147^{o}) and lower value of dielectric constant (2.0) than those of eugenol benzoxazine composites. Both cardanol and eugenol based benzoxazine coated cotton fabrics exhibit an excellent oil-water separation behavior. Similarly, cardanol based benzoxazine reinforced with natural fibrous materials namely rice husk, jute felt, coir felt and kapok fabric possess good sound absorption behavior. Data resulted from corrosion studies, it was noticed that the mild steel specimen coated with bio-based benzoxazine matrices and bio-silica reinforced benzoxazine composites coated specimens exhibit higher resistance towards corrosion. Results obtained from different studies, it is suggested that the bio-based composites developed in the present study can be used for some of the industrial applications viz., microelectronics insulation, oil-water separation, sound absorption and corrosion resistance uses. The present work is aimed to utilize renewable bio-source matrices and sustainable bio-based reinforcements to replace fossil fuel feed stocks to the extent possible to minimize environmental pollution.

Reference

[1] Á. L. Santana, M. Angela A. Meireles, New Starches are the Trend for Industry Applications: A Review, Food Public Heal. 4 (2014) 229–241. doi:10.5923/j.fph.20140405.04.

[2] H.P.S. Abdul Khalil, A.H. Bhat, A.F. Ireana Yusra, Green composites from sustainable cellulose nanofibrils: A review, Carbohydr. Polym. 87 (2012) 963–979. doi:10.1016/j.carbpol.2011.08.078.

[3] Y. Shen, C. Du, J. Zhou, F. Ma, Application of Nano FeIII-Tannic Acid Complexes in Modifying Aqueous Acrylic Latex for Controlled-Release Coated Urea, J. Agric. Food Chem. 65 (2017) 1030–1036. doi:10.1021/acs.jafc.6b05274.

[4] B. Tajeddin, Cellulose-Based Polymers for Packaging Applications, Lignocellul. Polym. Compos. Process. Charact. Prop. 9781118773 (2014) 477–498. doi:10.1002/9781118773949.ch21.

[5] V.K. Thakur, M.K. Thakur, P. Raghavan, M.R. Kessler, Progress in green polymer composites from lignin for multifunctional applications: A review, ACS Sustain. Chem. Eng. 2 (2014) 1072–1092. doi:10.1021/sc500087z.

[6] H. Yi, L.Q. Wu, W.E. Bentley, R. Ghodssi, G.W. Rubloff, J.N. Culver, G.F. Payne, Biofabrication with chitosan, Biomacromolecules. 6 (2005) 2881–2894. doi:10.1021/bm050410l.

[7] L. Zhou, L. Fan, X. Yi, Z. Zhou, C. Liu, R. Fu, C. Dai, Z. Wang, X. Chen, P. Yu, D. Chen, G. Tan, Q. Wang, C. Ning, Soft Conducting Polymer Hydrogels Cross-Linked and Doped by Tannic Acid for Spinal Cord Injury Repair, ACS Nano. 12 (2018) 10957–10967. doi:10.1021/acsnano.8b04609.

[8] M.F. Butler, A.H. Clark, S. Adams, Swelling and mechanical properties of biopolymer hydrogels containing chitosan and bovine serum albumin, Biomacromolecules. 7 (2006) 2961–2970. doi:10.1021/bm060133y.

[9] M. Hong, E.Y.X. Chen, Future Directions for Sustainable Polymers, Trends Chem. 1 (2019) 148–151. doi:10.1016/j.trechm.2019.03.004.

[10] B.G. Laycock, P.J. Halley, Starch Applications: State of Market and New Trends, Elsevier B.V., 2014. doi:10.1016/B978-0-444-53730-0.00026-9.

[11] X. Liu, R. Zhang, T. Li, P. Zhu, Q. Zhuang, Novel Fully Biobased Benzoxazines from Rosin: Synthesis and Properties, ACS Sustain. Chem. Eng. 5 (2017) 10682–10692. doi:10.1021/acssuschemeng.7b02650.

[12] M. V. Lomova, A.I. Brichkina, M. V. Kiryukhin, E.N. Vasina, A.M. Pavlov, D.A. Gorin, G.B. Sukhorukov, M.N. Antipina, Multilayer Capsules of Bovine Serum Albumin and Tannic Acid for Controlled Release by Enzymatic Degradation, ACS Appl. Mater. Interfaces. 7 (2015) 11732–11740. doi:10.1021/acsami.5b03263.

[13] H.P.S. Makkar, Protein Precipitation Methods for Quantitation of Tannins: A Review, J. Agric. Food Chem. 37 (1989) 1197–1202. doi:10.1021/jf00088a083.

[14] W. Qu, Y. Huang, Y. Luo, S. Kalluru, E. Cochran, M. Forrester, X. Bai, Controlled Radical Polymerization of Crude Lignin Bio-oil Containing Multihydroxyl Molecules for Methacrylate Polymers and the Potential Applications, ACS Sustain. Chem. Eng. 7 (2019) 9050–9060. doi:10.1021/acssuschemeng.9b01597.

[15] P. Sahariah, M. Másson, Antimicrobial Chitosan and Chitosan Derivatives: A Review of the Structure-Activity Relationship, Biomacromolecules. 18 (2017) 3846–3868. doi:10.1021/acs.biomac.7b01058.

[16] C. Voirin, S. Caillol, N. V. Sadavarte, B. V. Tawade, B. Boutevin, P.P. Wadgaonkar, Functionalization of cardanol: Towards biobased polymers and additives, Polym. Chem. 5 (2014) 3142–3162. doi:10.1039/c3py01194a.

[17] P. Froimowicz, C. R. Arza, L. Han, H. Ishida, Smart, Sustainable, and Ecofriendly Chemical Design of Fully Bio-Based Thermally Stable Thermosets Based on Benzoxazine Chemistry, ChemSusChem. (2016) 1921–1928. doi:10.1002/cssc.201600577.

[18] A. Hariharan, M. Kesava, M. Alagar, K. Dinakaran, K. Subramanian, Optical, electrochemical, and thermal behavior of polybenzoxazine copolymers incorporated with tetraphenylimidazole and diphenylquinoline, Polym. Adv. Technol. 29 (2018) 355–363. doi:10.1002/pat.4122.

[19] K. Kannan, S. Krishnan, M. Chavali, M. Alagar, Studies on thermal behavior of imidazole diamine based benzoxazines, J. Appl. Polym. Sci. 135 (2018) 1–11. doi:10.1002/app.46562.

[20] A. Hariharan, K. Srinivasan, C. Murthy, M. Alagar, A Novel Imidazole-Core-Based Benzoxazine and Its Blends for High-Performance Applications, Ind. Eng. Chem. Res. 56 (2017) 9347–9354. doi:10.1021/acs.iecr.7b01816.

[21] A. Muthukaruppan, H. Arumugam, S. Krishnan, K. Kannan, M. Chavali, A low cure thermo active polymerization of chalcone based benzoxazine and cross linkable olefin blends, J. Polym. Res. 25 (2018). doi:10.1007/s10965-018-1556-9.

[22] A. Hariharan, K. Srinivasan, C. Murthy, M. Alagar, Synthesis and characterization of a novel class of low temperature cure Benzoxazines, J. Polym. Res. 25 (2017). doi:10.1007/s10965-017-1423-0.

[23] H. Arumugam, S. Krishnan, M. Chavali, A. Muthukaruppan, Cardanol based benzoxazine blends and bio-silica reinforced composites: Thermal and dielectric properties, New J. Chem. 42 (2018) 4067–4080. doi:10.1039/c7nj04506a.

[24] S. Devaraju, K. Krishnadevi, S. Sriharshitha, M. Alagar, Design and Development of Environmentally Friendly Polybenzoxazine–Silica Hybrid from Renewable Bio-resource, J. Polym. Environ. 27 (2019) 141–147. doi:10.1007/s10924-018-1327-z.

[25] K. Krishnadevi, S. Devaraju, S. Sriharshitha, M. Alagar, Y. Keerthi Priya, Environmentally sustainable rice husk ash reinforced cardanol based polybenzoxazine bio-composites for insulation applications, Polym. Bull. (2019). doi:10.1007/s00289-019-02854-4.

[26] K. Krishnamoorthy, D. Subramani, N. Eeda, A. Muthukaruppan, Development and

characterization of fully bio-based polybenzoxazine-silica hybrid composites for low-k and flame-retardant applications, Polym. Adv. Technol. 30 (2019) 1856–1864. doi:10.1002/pat.4618.

[27] Y.E. Dogan, B. Satilmis, T. Uyar, Synthesis and characterization of bio-based benzoxazines derived from thymol, J. Appl. Polym. Sci. 47371 (2018) 1–10. doi:10.1002/app.47371.

[28] Štirn, A. Ručigaj, M. Krajnc, Characterization and kinetic study of Diels-Alder reaction: Detailed study on N-phenylmaleimide and furan based benzoxazine with potential self-healing application, Express Polym. Lett. 10 (2016) 537–547. doi:10.3144/expresspolymlett.2016.51.

[29] S. Krishnan, H. Arumugam, M. Chavali, A. Muthukaruppan, High dielectric, low curing with high thermally stable renewable eugenol-based polybenzoxazine matrices and nanocomposites, J. Appl. Polym. Sci. 136 (2019) 1–11. doi:10.1002/app.47050.

[30] Z.T. Khodair, A.A. Khadom, H.A. Jasim, Corrosion protection of mild steel in different aqueous media via epoxy/nanomaterial coating: Preparation, characterization and mathematical views, J. Mater. Res. Technol. 8 (2019) 424–435. doi:10.1016/j.jmrt.2018.03.003.

[31] C. Zhou, X. Lu, Z. Xin, J. Liu, Corrosion resistance of novel silane-functional polybenzoxazine coating on steel, Corros. Sci. 70 (2013) 145–151. doi:10.1016/j.corsci.2013.01.023.

[32] H.M. Hung, D.K. Linh, N.T. Chinh, L.M. Duc, V.Q. Trung, Improvement of the corrosion protection of polypyrrole coating for CT3 mild steel with 10-camphorsulfonic acid and molybdate as inhibitor dopants, Prog. Org. Coatings. 131 (2019) 407–416. doi:10.1016/j.porgcoat.2019.03.006.

[33] P. Ocón, A.B. Cristobal, P. Herrasti, E. Fatas, Corrosion performance of conducting polymer coatings applied on mild steel, Corros. Sci. 47 (2005) 649–662. doi:10.1016/j.corsci.2004.07.005.

[34] C. Zhou, X. Lu, Z. Xin, J. Liu, Y. Zhang, Polybenzoxazine/SiO2 nanocomposite coatings for corrosion protection of mild steel, Corros. Sci. 80 (2014) 269–275. doi:10.1016/j.corsci.2013.11.042.

[35] C.U. Atuanya, D.I. Ekweghiariri, C.M. Obele, Experimental study on the microstructural and anti-corrosion behaviour of Co-deposition Ni–Co–SiO2 composite coating on mild steel, Def. Technol. 14 (2018) 64–69. doi:10.1016/j.dt.2017.10.001.

[36] S.R. Nayak, K.N.S. Mohana, Corrosion protection performance of functionalized graphene oxide nanocomposite coating on mild steel, Surfaces and Interfaces. 11 (2018) 63–73. doi:10.1016/j.surfin.2018.03.002.

[37] R.M. Bandeira, J. van Drunen, G. Tremiliosi-Filho, J.R. dos Santos, J.M.E. de Matos, Polyaniline/polyvinyl chloride blended coatings for the corrosion protection of carbon steel, Prog. Org. Coatings. 106 (2017) 50–59. doi:10.1016/j.porgcoat.2017.02.009.

[38] M. Derradji, N. Ramdani, T. Zhang, J. Wang, L.D. Gong, X.D. Xu, Z.W. Lin, A. Henniche, H.K.S. Rahoma, W. Bin Liu, Effect of silane surface modified titania nanoparticles on the thermal, mechanical, and corrosion protective properties of a bisphenol-A based phthalonitrile resin, Prog. Org. Coatings. 90 (2016) 34–43. doi:10.1016/j.porgcoat.2015.09.021.

[39] Y. Li, Q. Yu, X. Yin, J. Xu, Y. Cai, L. Han, H. Huang, Y. Zhou, Y. Tan, L. Wang, H. Wang, Fabrication of superhydrophobic and superoleophilic polybenzoxazine-based cotton fabric for oil–water separation, Cellulose. 25 (2018) 6691–6704. doi:10.1007/s10570-018-2024-8.

[40] C. He, J. Huang, S. Li, K. Meng, L. Zhang, Z. Chen, Y. Lai, Mechanically Resistant and Sustainable Cellulose-Based Composite Aerogels with Excellent Flame Retardant, Sound-Absorption, and Superantiwetting Ability for Advanced Engineering Materials, ACS Sustain. Chem. Eng. 6 (2018) 927–936. doi:10.1021/acssuschemeng.7b03281.

List of Tables

Table 1. Thermal stability, dielectric constant and contact angle, of Poly(C-f)/bio-silica composites.

Sample	Thermal Stability			Water contact angle (^{o})	Dielectric constant (k)	Dielectric loss (*tan θ*)
	5% weight loss (^{o}C)	T_d (^{o}C)	Char yield % at 800^{o}C			
Neat poly(C-f)	362	463	4	98	3.61	0.0047
1 wt% bio-silica/ poly(C-f)	375	467	6	113	3.23	0.0045
3 wt% bio-silica/ poly(C-f)	379	470	10	124	2.73	0.0029
5 wt% bio-silica/ poly(C-f)	381	474	11	131	2.19	0.0029
7 wt% bio-silica/ poly(C-f)	387	478	12	147	2.00	0.0016

Table 2. Thermal stability, contact angle and dielectric constant of poly(E-f) and composites.

Sample	Thermal stability				Water contact angle (^{o})	Dielectric constant (k)	Dielectric loss (*tan θ*)
	5% weight loss (^{o}C)	T_d (^{o}C)	Char yield % at 800^{o}C	LOI			
Neat poly(E-f)	378	413	42	34.3	92	3.9	0.0055
1 wt% bio-silica/ poly(E-f)	382	417	45	35.5	96	3.2	0.0043
3 wt% bio-silica/ poly(E-f)	389	419	46	35.9	105	2.6	0.0037
5 wt% bio-silica/ poly(E-f)	395	426	51	37.9	118	2.3	0.0032
7 wt% bio-silica/ poly(E-f)	404	429	53	38.7	128	2.1	0.0021

Table 3. Corrosion parameters of the polybenzoxazines coated and bare mild steel specimens in 3.5 % NaCl solution from potentiodynamic polarisation studies.

Bio-silica weight (wt%)	Corrosion parameters			
	Rs (ohm cm^2)	CPE($F.s^{n-1}$)	N	R_{ct} / kΩ cm^2
poly(C-f)/ bio-silica coated specimen				
Bare MS	0.2021	$0.1123xe^{-3}$	0.877	150
0	0.2108	$0.354xe^{-3}$	0.742	151
1	1.332	$7.11xe^{-3}$	0.736	250
3	2.020	$1.787xe^{-3}$	0.807	270
5	2.891	$5.941xe^{-3}$	0.736	368
7	3.946	$4.593xe^{-3}$	0.564	403
Poly(E-f)/ bio-silica coated specimen				
0	0.254	$25.49xe^{-6}$	0.52	120
1	0.421	$1.925xe^{-3}$	0.774	171
3	0.589	$1.145xe^{-3}$	0.798	191
5	3.963	$0.104\ xe^{-3}$	0.775	300
7	4.066	$3.897xe^{-4}$	0.780	590

Table 4. Corrosion parameters of the polybenzoxazines coated and uncoated mild steel specimens in 3.5 % NaCl solution from Tafel studies.

Bio-silica reinforcement in wt %	E_{corr}(mV)	I_{corr} (µA)	CR mm year^{-1}	Efficiency η (%)
CF PBz/ bio-silica coated specimen				
Bare MS	-780	115	0.004455	0
0	-670	110	0.004261	4.32
1	-642	46	0.001782	60.00
3	-606	45	0.001588	60.86
5	-579	41	0.001743	64.34
7	-563	34	0.001317	75.00
Poly(E-f)/ bio-silica coated specimen				
0	-662	113	0.009026	1.73
1	-626	104	0.004029	9.52
3	-603	67	0.002595	41.73
5	-600	61	0.002363	46.95
7	-526	15	0.000891	87.00

Table 5. Mechanical behavior of poly(C-f) and poly(E-f) coated cotton fabrics.

Sample name	Porosity (µm)	Tensile Strength (N)		Elongation (%)	
		warp	weft	warp	weft
Non-coated cotton fabric	28.9	147.6	78.5	19.6	10.6
Poly (E-f) coated cotton fabric	26.1	169.9	86.2	20.9	11.4
Poly (C-f) coated cotton fabric	25.8	278.1	128.4	22.8	12.2

1

List of Scheme

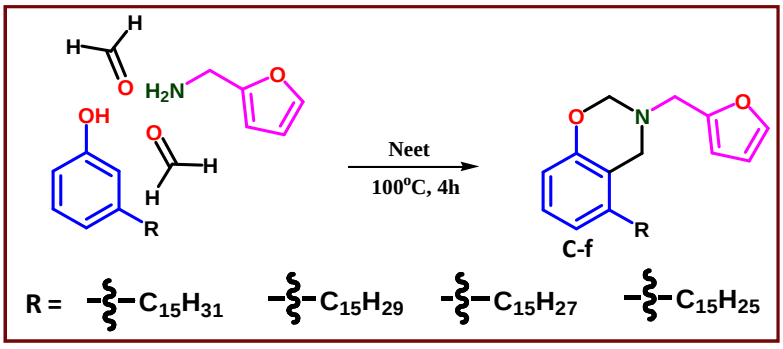

Scheme 1. Synthesis of cardanol- furfuryl amine based benzoxazine (C-f).

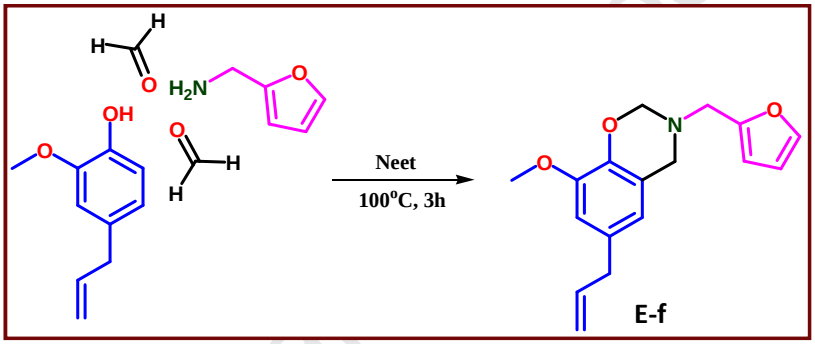

Scheme 2. Synthesis of eugenol- furfuryl amine based benzoxazine (Ef).

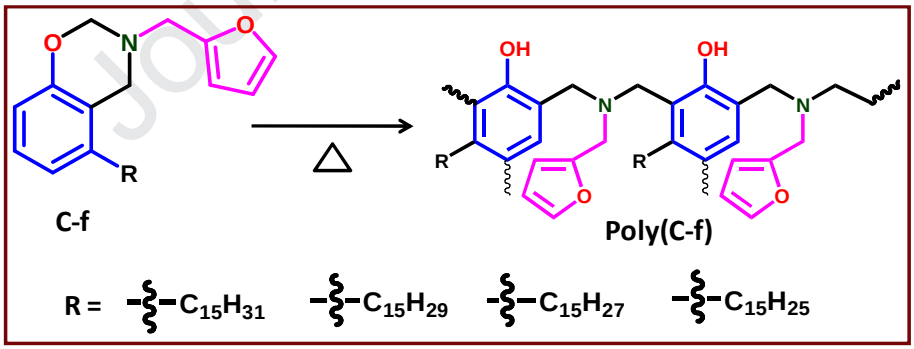

Scheme 3. Synthesis of cardanol- furfuryl amine based polybenzoxazine (poly(C-f)).

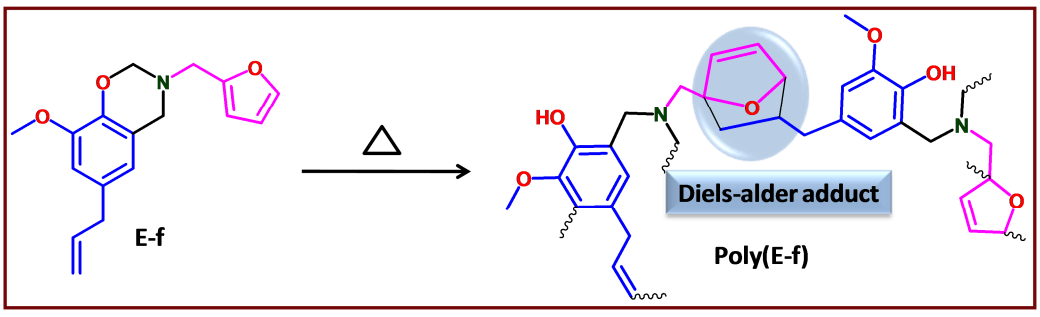

Scheme 4. Synthesis of eugenol- furfuryl amine based polybenzoxazine (poly(E-f)).

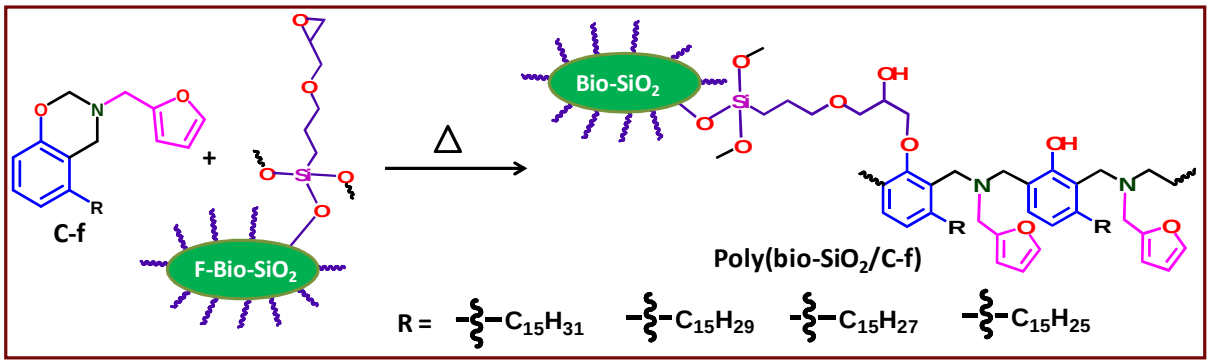

Scheme 5. Bio-silica reinforced poly(C-f) composites.

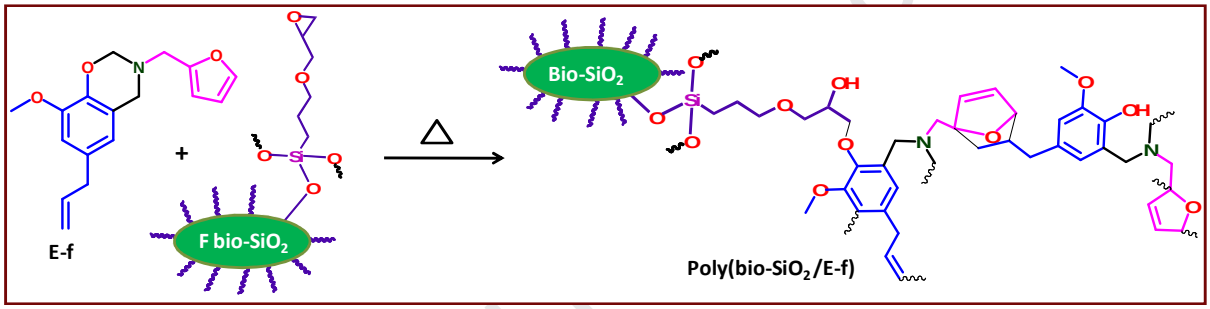

Scheme 6. Bio-silica reinforced poly(E-f) composites.

List of Figures

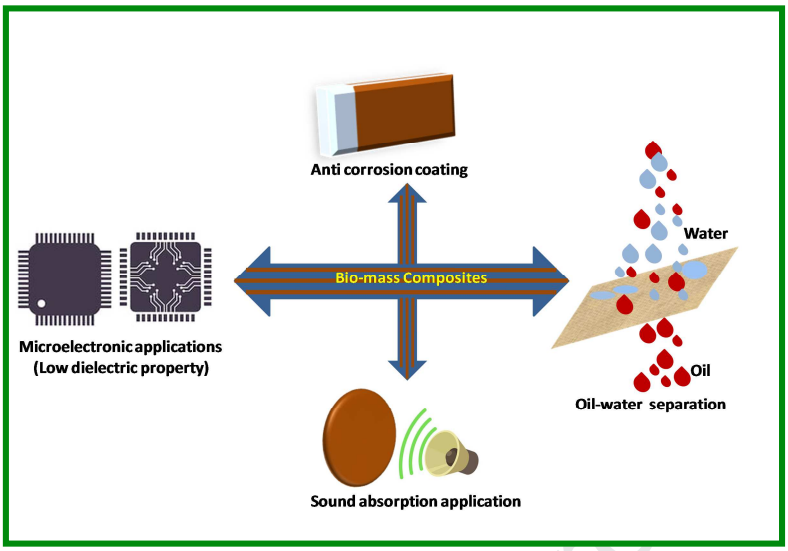

Figure. 1. Bio-mass composites for dielectric, corrosion resistance, sound absorption and oil water separation.

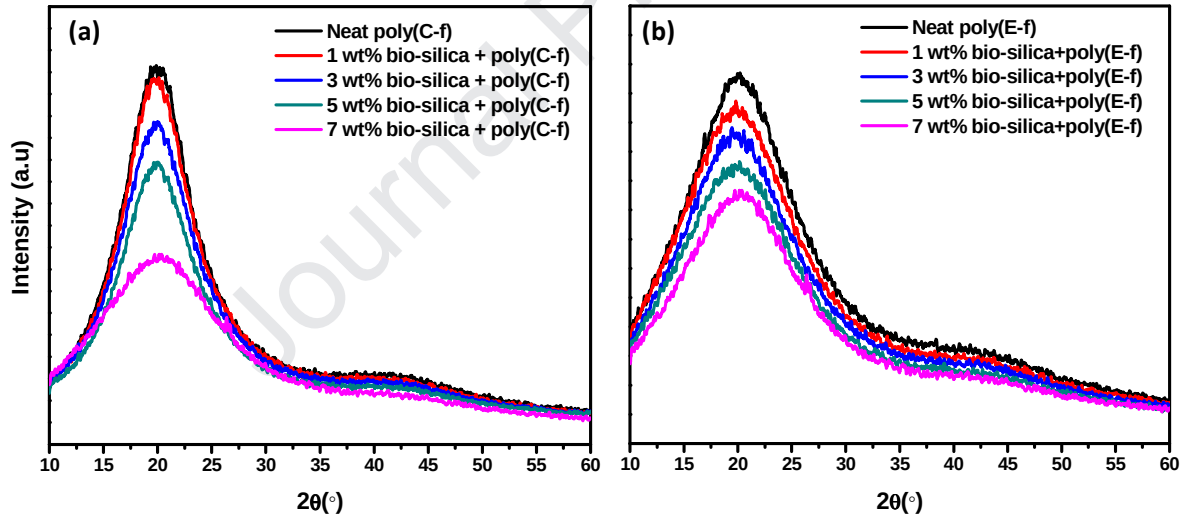

Figure. 2. XRD pattern of functionalized bio-silica reinforced (a) Poly(C-f) and (b) Poly(E-f) composites.

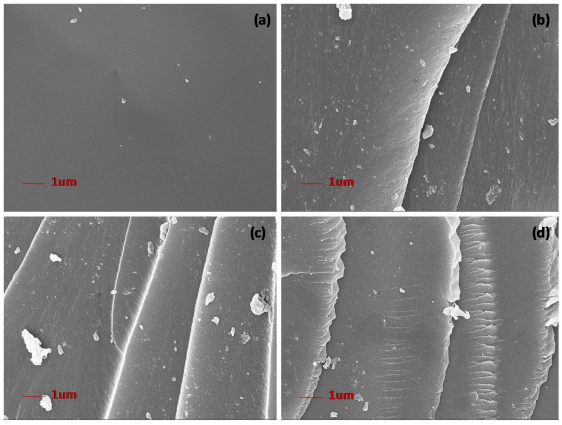

Figure. 3. SEM images of (a) 0 wt%, (b) 1 wt%, (c) 5 wt% and (d) 7wt% functionalized bio-silica reinforced Poly(C-f) composites.

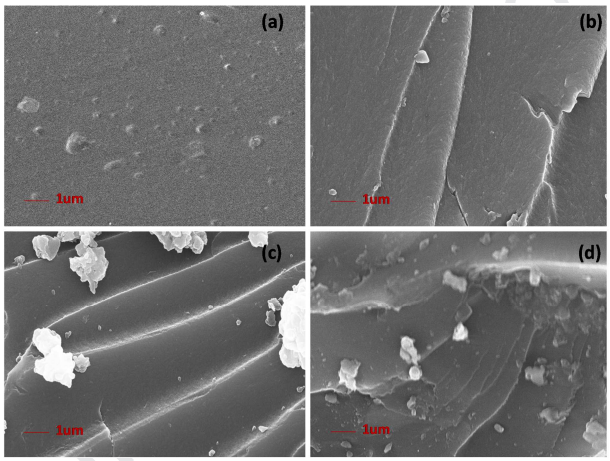

Figure. 4. SEM images of (a) 0 wt%, (b) 1 wt%, (c) 5 wt% and (d) 7wt% functionalized bio-silica reinforced Poly(E-f) composites.

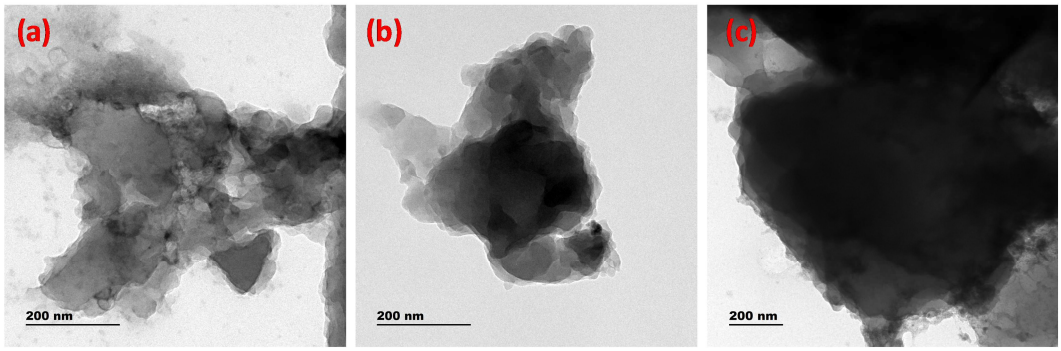

Figure. 5. TEM micrograph of (a) 3 wt%, (b) 5 wt%, (c) 7 wt% bio-silica reinforced Poly(C-f) nanocomposites.

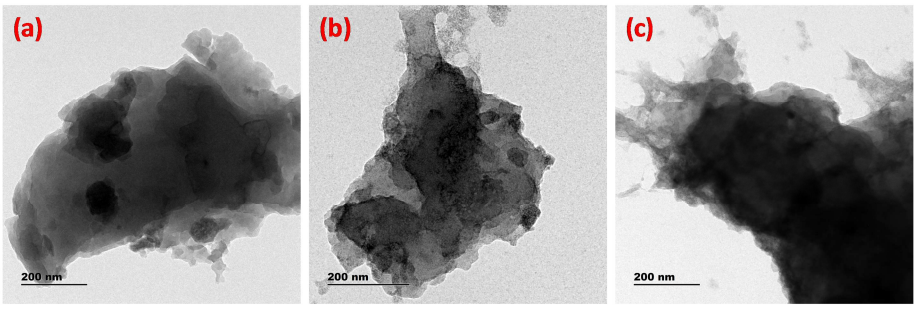

Figure. 6. TEM micrograph of (a) 3 wt%, (b) 5 wt%, (c) 7 wt% bio-silica reinforced Poly(E-f) nanocomposites.

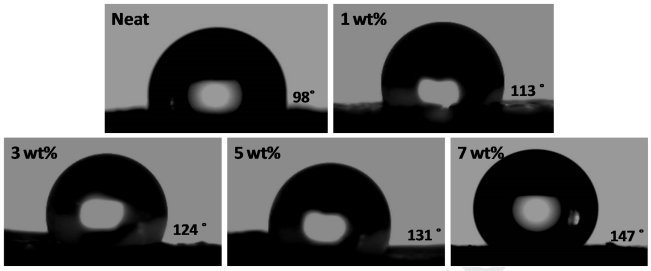

Figure. 7. Contact angle images of functionalized bio-silica neat, 1, 3, 5 and 7 wt% reinforced Poly(C-f) polybenzoxazine.

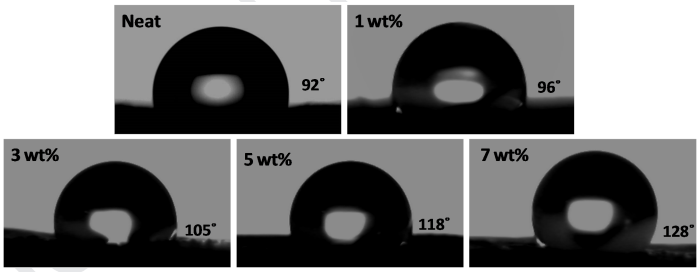

Figure. 8. Contact angle images of functionalized bio-silica 0, 1, 3, 5 and 7 wt% reinforced Poly(E-f) polybenzoxazine.

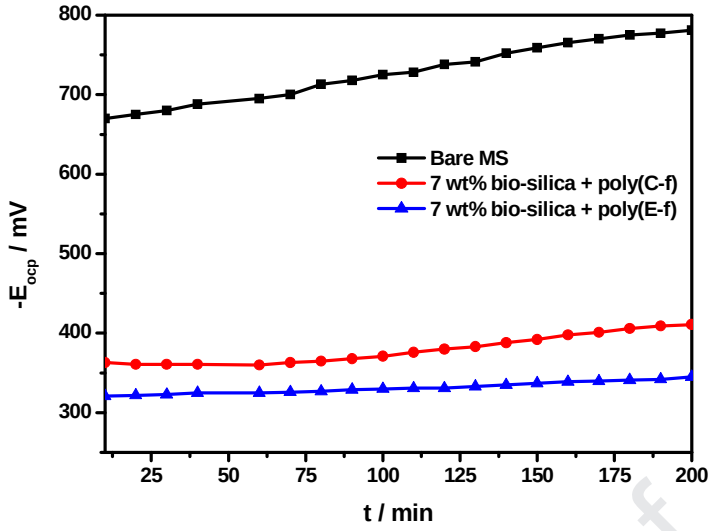

Figure. 9. Plot of E_{ocp} Vs immersion time in 3.5 % NaCl solution for bare MS and 7 wt% bio-silica reinforced Poly(C-f) and Poly(E-f) composites.

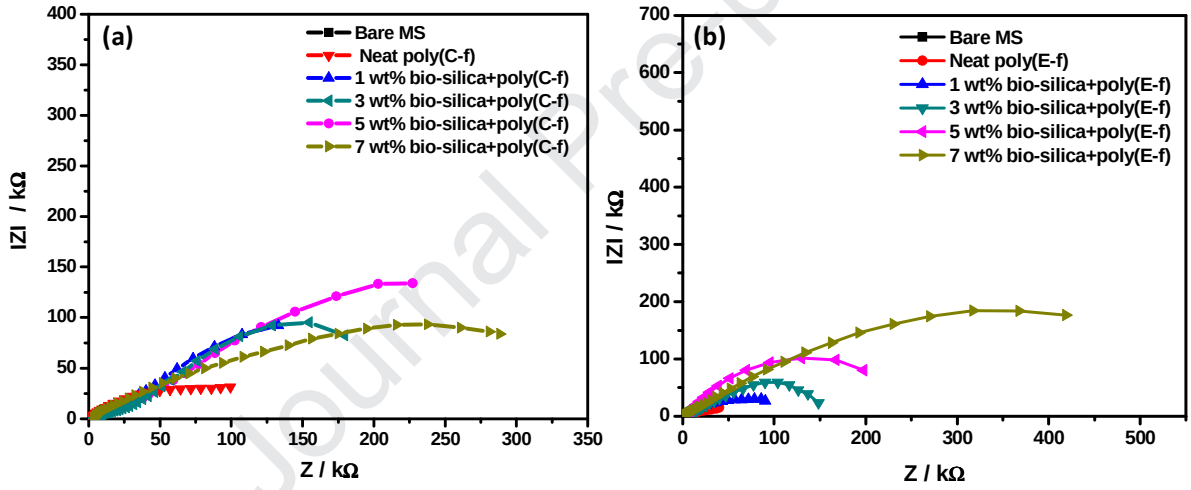

Figure. 10. EIS response of bare MS and bio-silica reinforced benzoxazine composite (a) Poly(C-f) composites (b) Poly(E-f)composites coated specimens in 3.5% NaCl solution.

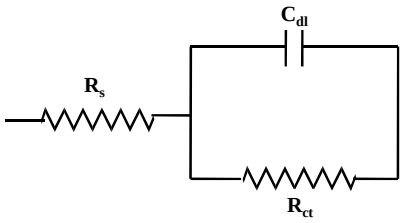

Figure. 11. The equivalent circuit used for impedance analysis.

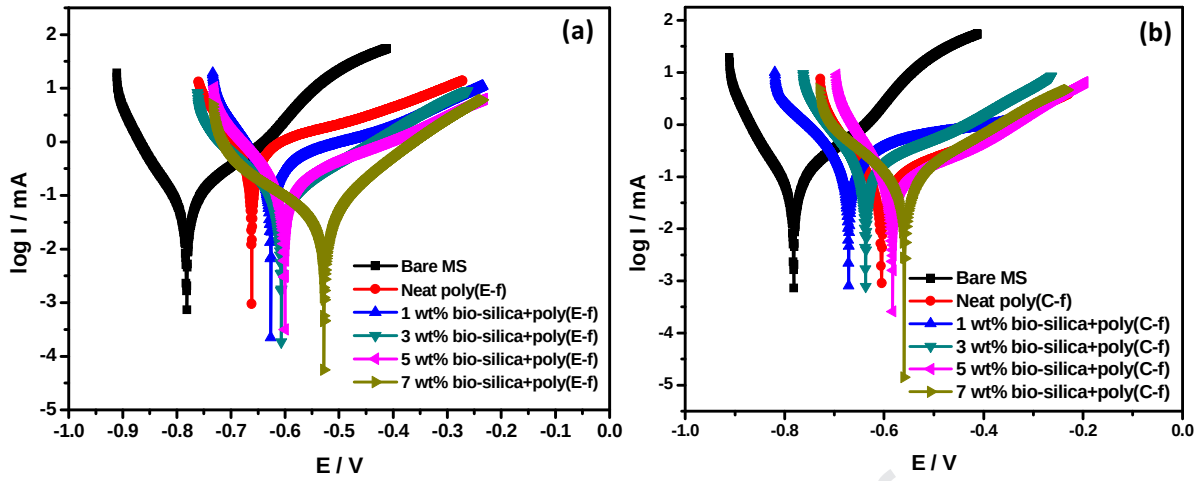

Figure. 12. Tafel plots of bare MS and bio-silica reinforced benzoxazine composites (a) Poly(C-f) / bio-silica composites (b) Poly(E-f)/ bio-silica composites coated specimens in 3.5% NaCl solution.

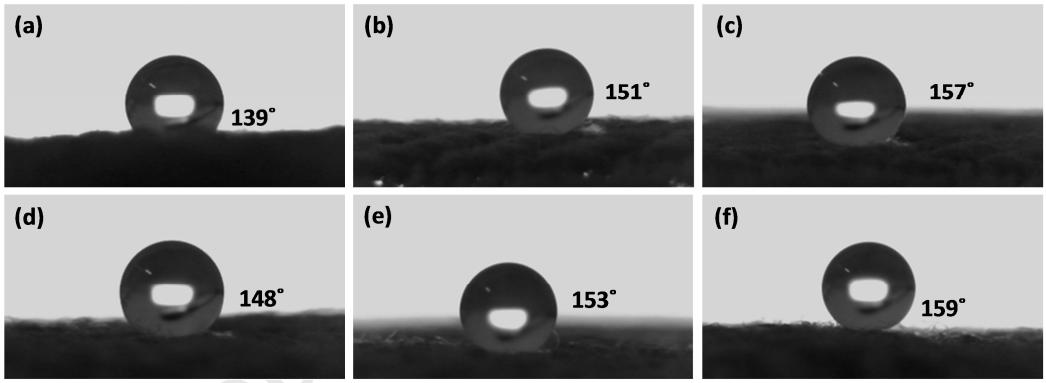

Figure. 13. The water contact angle of benzoxazines coated cotton fabrics (a) 15 wt% CF-bz, (b) 10 wt% (c) 5 wt% loaded Poly(C-f) on cotton fabrics, (d) 15 wt% Poly(E-f), (e) 10 wt% (f) 5 wt% loaded Poly(E-f) on cotton fabrics.

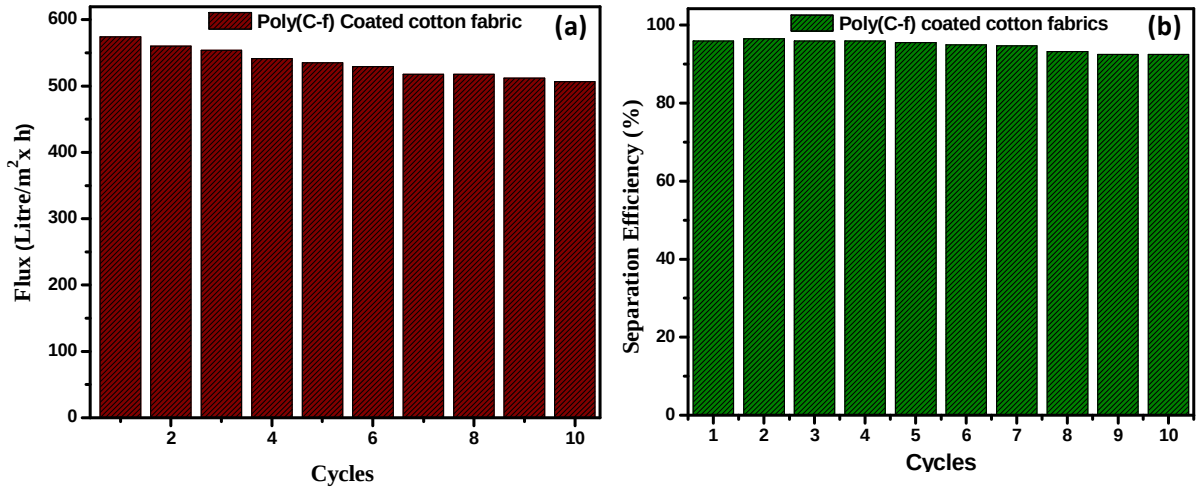

Figure. 14. Oil-water (a) separation efficiency and (b) flux of Poly(C-f) coated cotton fabrics.

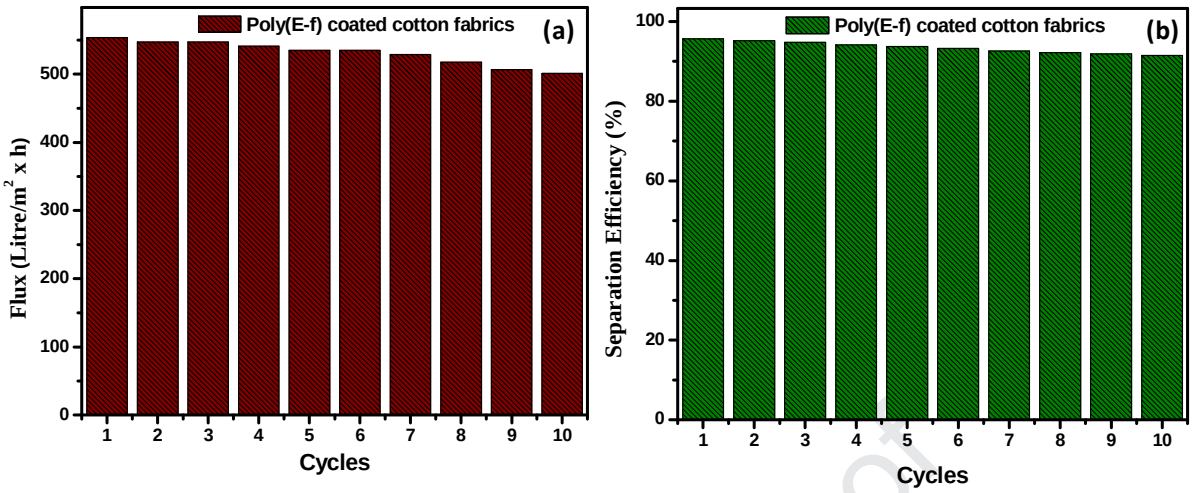

Figure. 15. Oil-water (a) separation efficiency and (b) flux of Poly(E-f) coated cotton fabrics.

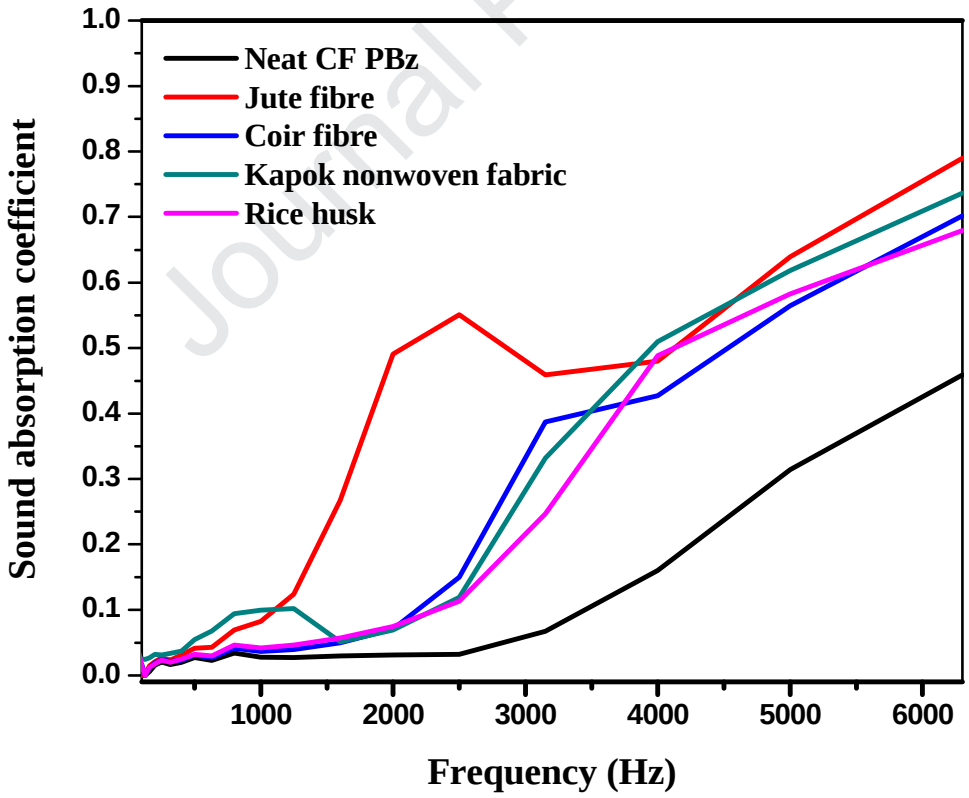

Figure. 16. Sound absorption coefficient of Poly(C-f) composites with natural fibers.

Highlights

Bio-based polybenzoxazine composites for oil-water separation, sound absorption and corrosion resistance applications.

Arumugam Hariharan[a], Pichaimani Prabunathan[a], Ammasai Kumaravel[b], Manickam Manoj[a], Muthukarupan Alagar[a]*

[a]Polymer Engineering Laboratory, PSG Institute of Technology and Applied Research, Neelambur, Coimbatore - 641 062, India.
[b]Department of Chemistry, PSG Institute of Technology and Applied Research, Neelambur, Coimbatore - 641 062, India.
*Corresponding author: mkalagar@yahoo.com

- Bio-composite derived from bio-mass based benzoxazines and reinforcements have been explored for industrial application.
- Bio-silica reinforced polybenzoxazine composites have been studied for their insulation behavior and corrosion resistant efficiency.
- Bio-based benzoxazines coated cotton fabrics were studied for oil-water separation behavior.
- Natural fiber such as rice-husk, coir felt, jute felt and kapok reinforced bio-benzoxazine composites were studied for their sound absorption behavior.

Graphical Abstract

Bio-benzoxazine composites for oil-separation and sound absorption applications.

Arumugam Hariharan[a], P. Prabunathan[a], A. Kumaravel[b], Manickam Manoj[a], Muthukarupan Alagar[a]*

[a]Polymer Engineering Laboratory, PSG Institute of Technology and Applied Research, Neelambur, Coimbatore - 641 062, India.
[b]Department of Chemistry, PSG Institute of Technology and Applied Research, Neelambur, Coimbatore - 641 062, India.

*Corresponding author: mkalagar@yahoo.com

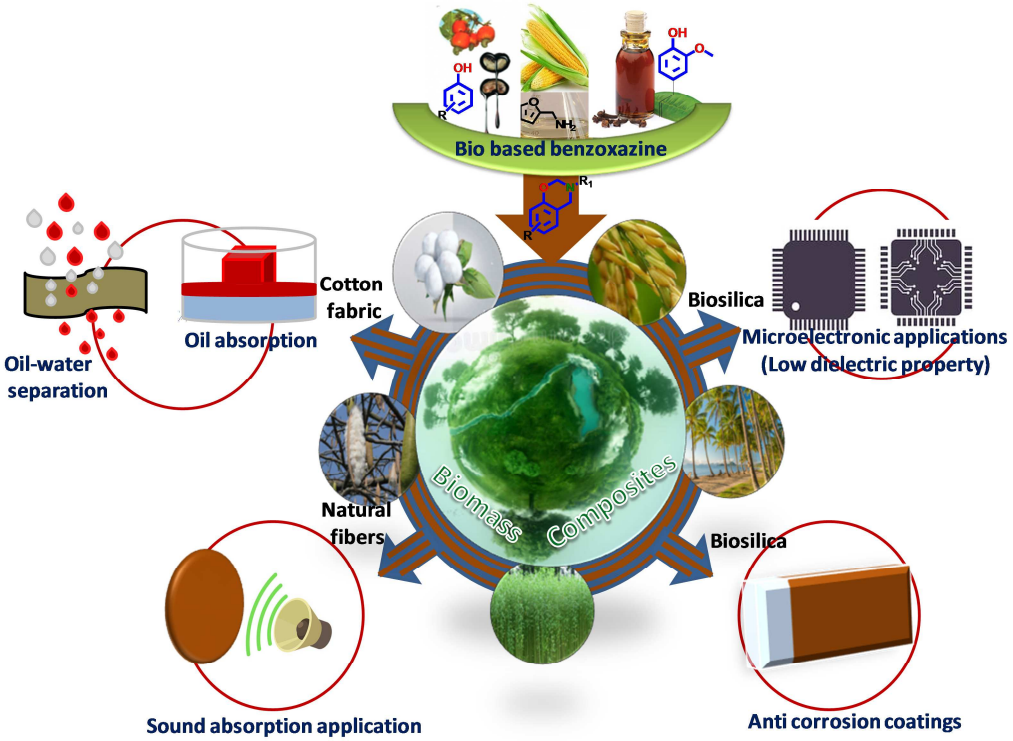

The super hydrophobic behavior of bio-composites utilized for low k, corrosion resistance, oil water separation, and sound absorption applications.

Conflicts of interests

There are no conflicts to declare.